

Investigation of the plasma properties and plasma-generated reactive species using optical spectroscopy in microwave-excited atmospheric pressure Ar microplasma jets

Jae Keun Park, Yang Won Kwon, Hea Min Joh, and T. H. Chung

¹⁾ *Department of Physics, Dong-A University, Busan 49315, Korea*

Abstract:

An atmospheric pressure plasma jet was generated by a microwave source utilizing coaxial transmission line resonator. We investigated the effects of the operating parameters such as input power, excitation frequency, and gas flow rate on the plasma properties such as electron density and electron temperature using optical emission spectroscopy. And the amounts of various reactive species in the plasma-treated liquids were estimated using ultraviolet absorption spectroscopy, chemical probe method, and UV-VIS spectrophotometry.

Keywords: microwave-excited plasma, atmospheric pressure plasma jets, electron temperature, reactive oxygen species

1. Introduction

Since atmospheric pressure plasma jets (APPJs) can produce non-thermal plasma containing reactive species, their applications have rapidly expanded to biology and medicine [1 - 3]. The use of APPJs in biomedical applications is drawing considerable attention because plasmas contain short lived free radicals, including reactive oxygen and nitrogen species (RONS), charged species, and electric fields. In particular, microwave-excited APPJs have several advantages over low-frequency plasmas: high density of electron and reactive species, low breakdown power, low heavy-particle temperature, and lower discharge voltages [4 - 6]. One of the most important factors is the plasma-generated reactive species including RONS. The operating parameters of microwave-excited APPJs (input power, driving frequency, and gas flow rate of APPJs) influence the generation of RONS in the gas phase and in the plasma-treated liquid. Non-intrusive spectroscopic diagnostics are useful choices to investigate the plasma properties of APPJs. In this work, the electron density and electron temperature were estimated via optical emission spectroscopy using various interpretation methods [7 - 10]. The RONS generated in both the gas phase and the liquid phase were measured using different diagnostic methods such as optical emission spectroscopy, ultraviolet absorption spectroscopy [11], chemical probe method [12], and UV-VIS spectrophotometry [13].

2. Materials and methods

The experimental setup is shown in Fig. 1. The plasma was generated by a microwave-excited micro-plasma source that uses a coaxial transmission line resonator (CTLR) operating at around 780 MHz. A signal generator (Agilent E8251A) and a linear power RF amplifier

(OPHIR RF 5016A) were used to supply power to the CTLR. The incident and reflected powers were monitored using two directional couplers (CK-68N), power sensors (E9300A) and power meters (E4416A). Microwave power up to 10 W was supplied directly to the CTLR from the signal generator and power amplifier. The optical emission spectrum of the APPJ was measured using two kinds of spectrometers; a photodiode-array spectrometer (Ocean Optics USB2000+XR1-ES), and monochromator (SPEX 1702) with a photomultiplier tube (PMT) (Hamamatsu R928)). The gas temperature T_G was measured using a fiber-optic temperature sensor (Luxtron M601-DM&STF). The operating conditions included various gas flow rates (2.5, 3.0, 3.5 L/min), input powers (3 - 5 W), and driving frequency (780 MHz, 2.45 GHz) with argon gas.

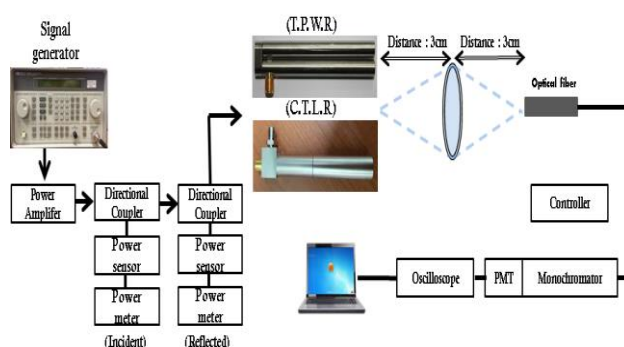


Fig. 1. Experimental setup.

NO was measured by a tube-type gas detector (KITAGAWA AP-20). Ozone generation was detected using an ozone detector (2B Technologies Model 202) that is based on the well-established technique of

absorption of UV light at 254 nm.

The generated RONS were measured at the liquid phase by UV absorption spectroscopy [11] and compared with those present in the gas phase measured by optical emission spectroscopy. The OH concentration in the liquid was also measured by a chemical probe method using TA solution [12]. Some long-lived RONS including H₂O₂, NO₃⁻ and NO₂⁻ are readily generated by plasma contacting the liquid. The concentration of H₂O₂, NO₂⁻, NO₃⁻, and O₃ in plasma-treated media was detected after plasma treatment at different time points by using Spectrophotometer (Photolab® 7600 UV-VIS series, WTW GmbH, Germany) [13]. The measurement of nitrite concentration was also obtained by Griess assay [14].

3. Electron temperature and electron density

Electron temperature (T_e) can be estimated by optical emission spectroscopy under several methods [7 – 9]. In particular, the excitation temperature (T_{exc}) of $2p$ and $3p$ levels has been used to estimate T_e in an atmospheric-pressure discharge. In these discharges, since the electron-atom collisions and atom-atom collisions are the most important processes for these levels, T_{exc} increases with T_e [15]. T_{exc} can be determined from a Boltzmann plot, which is obtained from the measurement of emission intensity and λ of Ar $3p \rightarrow 1s$ and $2p \rightarrow 1s$ peaks. We observed that the Ar population distribution over the energy levels is compatible with the Boltzmann distribution in our experimental conditions. Therefore, the Boltzmann-plot method can be used to calculate T_{exc} . The T_{exc} may be used as a rough indication of the electron temperature [10]. The results suggest that the microwave-excited APPJ can achieve higher mean electron energy than that in low-frequency APPJs. The calculated T_{exc} was in the range of 0.5 ~ 1.2 eV. Change in the input power did not affect T_{exc} much, but increase in the gas flow rate caused slight decrease in T_{exc} , possibly due to an effective increase of the air mixing, which causes an increase in the frequency of electron-neutral collisions.

The second simple method assumes that the direct excitation from the ground state with radiative decay dominates over the production and destruction of excited energy levels. For instance, many excited states of argon are mainly produced by electron-impact excitation from the ground state, and the quenching rate of excited argon atoms by Ar atoms is very small compared to the radiative decay [7]. This simplification is called the corona balance and expressed in a modified Boltzmann formula as follows:

$$\ln \left(\frac{\lambda_{ij} I_{ij} \sum_{i>j} A_{ij}}{R_{ij} A_{ij} a_{li}} \right) = - \frac{E_i}{k_B T_e} + C \quad (1)$$

where, I_{ij} , λ_{ij} , R_{ij} and A_{ij} are the intensity, wavelength, detector efficiency, and the Einstein coefficient of the spectral line from transition of $i \rightarrow j$ level, respectively. The a_{li} is the coefficient in an exponential approximation of electron impact excitation rate coefficient from ground state to level i , k_B is the Boltzmann constant, and E_i is the excitation energy of level i [7]. A modified Boltzmann plot (Eq. (1)) was drawn from many Ar peaks at 750.4 nm ($2p_1 \rightarrow 1s_2$), 811.5 nm ($2p_9 \rightarrow 1s_5$), 696.5 nm ($2p_2 \rightarrow 1s_5$), 706.7 nm ($2p_3 \rightarrow 1s_5$), 738.3 nm ($2p_3 \rightarrow 1s_4$), 763.5 nm ($2p_6 \rightarrow 1s_5$), 772.4 nm ($2p_2 \rightarrow 1s_3$), 794.8 nm ($2p_4 \rightarrow 1s_3$), 810.4 nm ($2p_7 \rightarrow 1s_4$), and 801.4 nm ($2p_8 \rightarrow 1s_5$).

The third method assumes that population of $2p$ excited argon levels mainly occurs by electron collision with argon atoms in the ground level and with atoms in the metastable levels ($1s_3$ and $1s_5$) and that depopulation process from $2p$ levels are represented by radiative decay to $1s$ states [8]. If we assume that the electrons follow a Maxwell-Boltzmann energy distribution, then we can determine the electron temperature from the balance equation.

Zhu *et al.* proposed a more detailed collisional-radiative model for atmospheric-pressure low-temperature argon discharges [9]. In this model, the population ratios of $2p_1$ and $2p_3$ can be calculated as functions of electron density. Electron density can be determined from the intensity ratio of emission lines, $I_1 (= A_1 n_{2p1})/I_3 (= A_3 n_{2p3})$, from the excited levels $2p_1$ and $2p_3$.

The electron density can also be measured by the Stark broadening of the Balmer transition (4-2) of atomic hydrogen at 486.13 nm (H_β line) [16]. The H_β spectral line profile was measured and the Voigt profile was fitted to the experimental points. The fitting was made using the Voigt function with a Gaussian line width of 0.23 nm (in our typical case, $\Delta\lambda_1 = 0.22$ nm, $\Delta\lambda_D$ (Doppler broadening) = 0.008 nm ($T_g = 750$ K), $\Delta\lambda_V$ (FWHM of Voigt profile) = 0.315 nm). The shape and the FWHM of the instrumental broadening $\Delta\lambda_1$ were deduced by recording the Ne line (633 nm) emitted by a He-Ne laser. The resulting value of the FWHM of the Lorentzian profile $\Delta\lambda_L (= \Delta\lambda_{vdw}$ (Van der Waals broadening) + $\Delta\lambda_S$ (Stark broadening)) enabled us to calculate the electron number density n_e in Ar plasma. We can simply use the $\Delta\lambda_S$ [nm] which is related to n_e [cm⁻³] by [17] ($\Delta\lambda_S = 2.0 \times 10^{-11} n_e^{2/3}$). In our typical case, we have $\Delta\lambda_L = 0.147$ nm and $\Delta\lambda_{vdw} = 0.057$ nm, then we obtain $\Delta\lambda_S = 0.09$ nm. Calculated n_e using Ref. [17] has a value of 2.7×10^{14} cm⁻³.

4. Discussions and Conclusion

It turned out that in microwave-excited argon APPJ the excitation temperature is lower than the electron temperature, but both temperatures vary similarly with the input power and gas flow rate. The electron temperature obtained by the second (based on the corona balance) and the third methods provide comparable values, while the second method gave a little smaller value than that from

the third method. This can be explained by that the third model is more elaborate taking into account collisional excitation from metastable states. At a fixed input power, a lower gas flow rate makes a slightly higher electron temperature, electron density and gas temperature. However, increasing power will mainly cause an expansion of the discharge volume and a slight rise in the electron density, while leaving the electron temperature more or less unchanged. Results of the line ratio method to obtain the electron density in microwave-excited APPJs are found to be in agreement with those of the Stark broadening method. The OES peaks from OH, O, and NO were observed to increase slightly with the input power, similar to the change of the electron density with the input power. The changes of NO and O₃ concentrations with the input power and gas flow rate were monitored and compared with the emission intensities of OH, O, and NO.

The consequences of operating parameters (input power, gas flow rate, and driving frequency) on the RONS production were investigated. The RONS in the gas phase depended on the plasma-exposure time, input power, and gas flow rate. The RONS in the plasma-treated liquid also depended on the gas temperature thus making their dependence on the operating parameters in a complicated manner.

The changes in the RONS concentration in the gas phase with varying operating parameters exhibited similarly to those of the plasma-treated liquids. The results are very suggestive that there is a strong correlation among the production of RONS in the plasmas and liquids.

This work was supported by the National Research Foundation of Korea (NRF) under contract No. 2018R1D1A1A09081763.

5. References

- [1] M. Keidar, *Plasma Sources Sci. Technol.* **24**, 033001 (2015).
- [2] R. Miotk, B. Hrycak, D. Czyłkowski, M. Dors, M. Jasinski, and J. Mizeraczyk, *Plasma Sources Sci. Technol.* **25**, 035022 (2016).
- [3] A. R. Hoskinson, A. Yared, and J. Hopwood, *Plasma Sources Sci. Technol.* **24**, 055002 (2015).
- [4] H. Wk. Lee, S. K. Kang, I. H. Won, H. Y. Kim, H. C. Kwon, J. Y. Sim, and J. K. Lee, *Phys. Plasmas* **20**, 123506 (2013).
- [5] K. McKay, F. Iza, and M. G. Kong, *Eur. Phys. J. D* **60**, 497 (2010).
- [6] J. Gregório, A. R. Hoskinson, and J. Hopwood, *J. Appl. Phys.* **118**, 083305 (2015).
- [7] J. Gordillo-Vazquez, M. Camero and C. Gomez-Aleixandre, *Plasma Sources Sci. Technol.* **15** 42 (2006).
- [8] D. Mariotti, Y. Shimizu, T. Sasaki, and N. Koshizaki, *Appl. Phys. Lett.* **89**, 201502 (2006).
- [9] X. M. Zhu, Y. K. Pu, N. Balcon, and R. Boswell, *Phys. D: Appl. Phys.* **42** 142003 (2009).
- [10] J. L. Walsh and M. G. Kong, *Appl. Phys. Lett.* **93**, 111501 (2008).
- [11] E. J. Szili, J.-S. Oh, S.-H. Hong, A. Hatta, and R. D. Short, *J. Phys. D: Appl. Phys.* **48**, 202001 (2015).
- [12] K. Ninomiya T. Ishijima, M. Imamura, T. Yamahara, H. Enomoto, K. Takahashi, Y. Tanaka, Y. Uesugi, and N. Shimizu, *J. Phys. D: Appl. Phys.* **46**, 425401 (2013).
- [13] J. Ma, H. Zhang, C. Cheng, J. Shen, L. Bao, and W. Han, *Plasma Process Polym.* **14**, e1600162 (2017).
- [14] A. R. Gibson, H. O. McCarthy, A. A. Ali, D. O'Connell, and W. G. Graham, *Plasma Process. Polym.* **11**, 1142 (2014).
- [15] X. M. Zhu, W. C. Chen, and Y. K. Pu, *J. Phys. D: Appl. Phys.* **41** 105212 (2008).
- [16] G. Wattieaux, M. Yousfi, and N. Merbahi, *Spectrochimica Acta Part B* **89**, 66 (2013).
- [17] X.-M. Zhu, W.-C. Chen, and Y.-K. Pu, *J. Phys. D: Appl. Phys.* **41**, 105212 (2008).